Hard vs. Soft Physics at RHIC - Insights from PHENIX

B. V. Jacak For the PHENIX Collaboration
Department of Physics and Astronomy, SUNY Stony Brook,
Stony Brook NY, 11794

I. INTRODUCTION

Heavy ion collisions at high energies include physics processes at a variety of energy scales. The hadronic final state of heavy ion collisions, which is responsible for the bulk of the particle production, is dominated by "soft" processes. This state can be described as a thermal system with a temperature near 200 MeV. The data provide evidence for collective radial flow of the matter, which gives a boost to the transverse momentum spectra. "Hard" processes, on the other hand, occur early in the collision, with large momentum transfer scattering among the partons in the incoming nuclei. These partonic interactions create useful probes, which pass through the early, hottest phase of the collision. In particular, the charmonium bound state J/ψ, open charm, and jets are promising signals of quark-gluon plasma formation and properties. Production rates and distributions of these signals are calculable with perturbative QCD, and are sensitive to the evolution of the parton distribution as the nuclear collision proceeds. A major challenge at RHIC is to constrain which type of theoretical tools - QCD or thermal collective descriptions, such as hydrodynamics - can be used to describe which part of the particle spectra.

The PHENIX experiment was designed to measure a broad variety of signals from both heavy ion and polarized proton-proton collisions at RHIC. The penetrating probes from early stages of the collision, together with hadron measurements, require a detector capable of measuring observables sensitive to all stages of the collision process. Thus it is natural to use PHENIX to determine the boundary between hard and soft physics at RHIC. The PHENIX detector consists of three spectrometers: a central spectrometer with two arms each covering 90 degrees in azimuth with $|\eta| < 0.35$, and two muon spectrometers covering full azimuth for $1.1 < |\eta| < 2.4$. The central arms contain three tracking sub-systems: drift chambers (DC), pad chambers (PC) and time-expansion chambers (TEC), two types of electromagnetic calorimeter (PbGl and PbSc), a time-of- flight hodoscope (TOF) and ring imaging Cerenkov counters (RICH). Together with an axial field central magnet, and a set of beam-beam counters (BBC) located at $3 < |\eta| < 3.9$, these provide superb hadron and electron identification over a broad range of transverse momenta.[1] The data presented here are from Au+Au collisions at $\sqrt{s_{NN}} = 130$ GeV, measured in the central spectrometer in late summer 2000.

Collisions are sorted according to centrality using the correlation between the beam-beam counters and pulse height in the zero-degree calorimeters.[2] Pattern recognition to find tracks is based on a combinatorial Hough transform of drift chamber hits in the track bend plane; the polar angle of the track is determined by PC1 and the location of the collision z-vertex. A field integral look-up table is used to determine the charged particle momentum and the path length to the TOF detector located 5.06m from the beam line. The momentum resolution is $\delta p/p \approx 0.6\% \oplus 3.6\%$ p, and the timing resolution is approximately 115 ps.[3] Combining the momentum and flight time, we reconstruct the particle mass and identify hadrons by applying 2σ momentum dependent cuts in mass-squared; the quality of the particle identification is clear from Figure 1. Electrons are identified using the RICH and the EMCAL. The RICH, filled with 1 atm CO_2 radiator, detects an average of 10.8 photo-electrons per electron track, while a pion with $p < 4.7$ GeV/c produces no signal in the RICH. A clear electron signal is observed as a narrow peak centered at 1.0 in the E/p ratio, where E is the energy measured by the EMCAL and p is the momentum. We select tracks with $0.8 < E/p < 1.5$ as electrons. Corrections for acceptance, decays, momentum resolution and reconstruction efficiency are made using a full GEANT Monte Carlo simulation. Multiplicity dependent efficiencies were evaluated by embedding simulated tracks into real events.

II. PARTICLE PRODUCTION

PHENIX observes $dN_{ch}/d\eta_{|\eta=0} = 609 \pm 1(\text{stat}) \pm 37(\text{syst})$,[2] in the most central collisions, in good agreement with values reported by other experiments. This value reflects an increase with $\sqrt{s}$ much larger than observed in $p-p$ and $p-\overline{p}$ collisions, and suggests that some of the increase may be due to multiple low momentum particles arising when partons traversing the early, dense part of the collision lose energy.[4]

Models, such as HIJING [4] or the gluon saturation model discussed by Kharzeev and Nardi,[5] predict that there is a component of particle production from soft interactions that scales linearly with the number of participant nucleons, N_{part}, and a hard component which includes a term scaling with the number of collisions, N_{coll}. The centrality

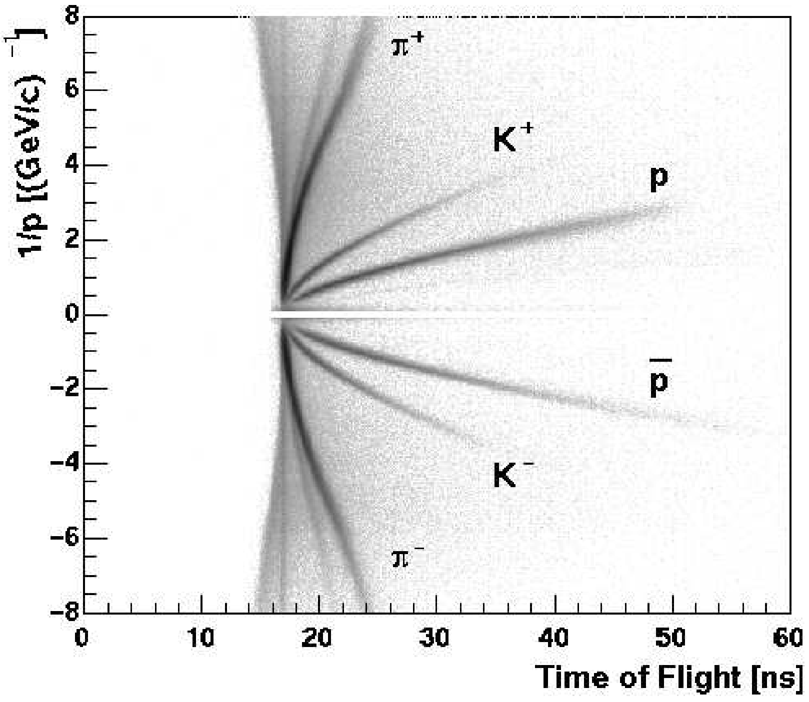

FIG. 1: Particle identification by time of flight in PHENIX. The measured time of flight is plotted vs. the inverse of the momentum.

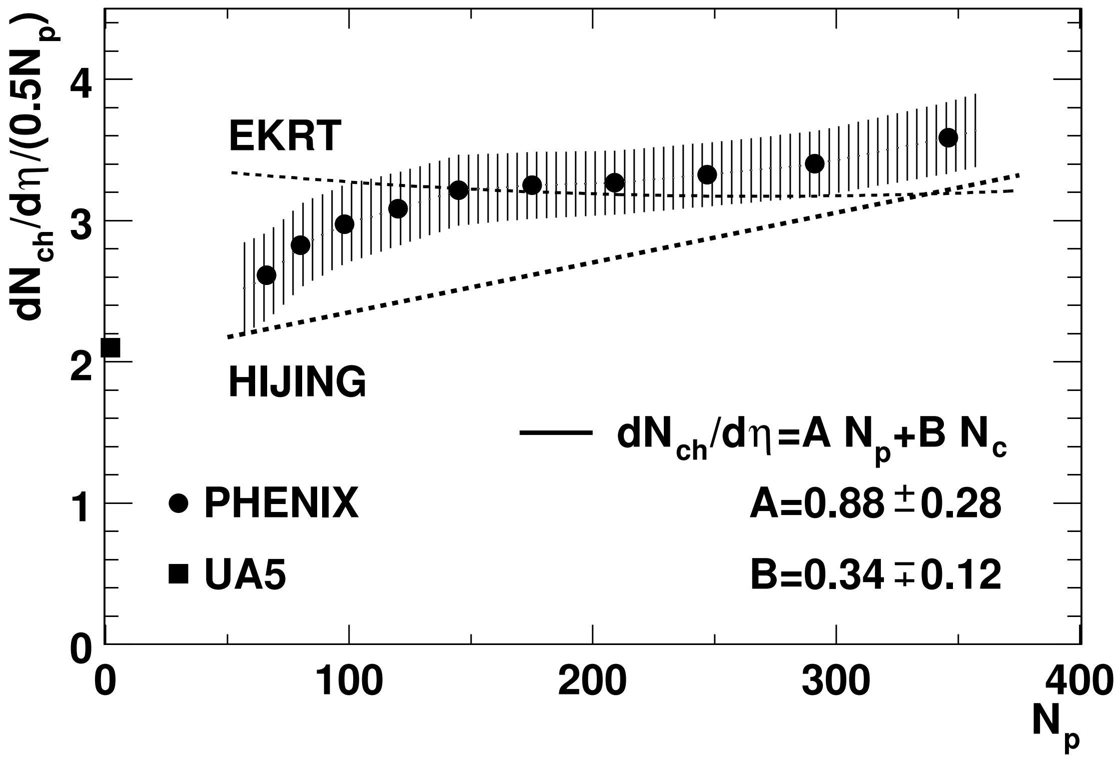

FIG. 2: Charged particle rapidity density, as function of the number of participant nucleon pairs. Predictions from the HIJING and EKRT models, along with a simple phenomenological fit are also shown. The shaded area represents the systematic errors on the charged particle measurement and N_{part}.

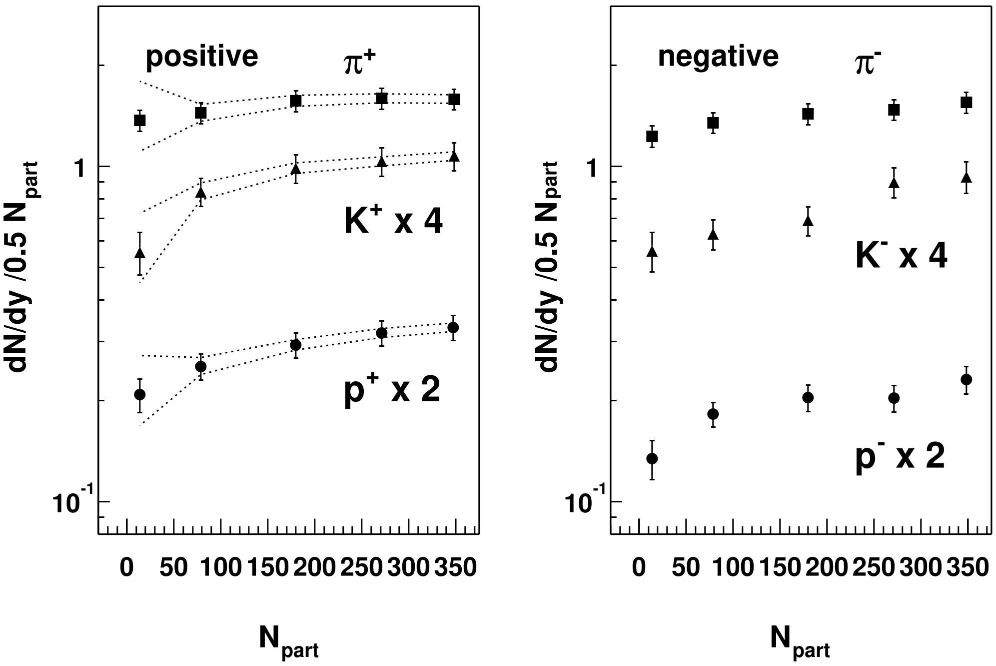

FIG. 3: Hadron yields per participant nucleon in Au+Au, as a function of the number of participants. The error bars indicate statistical errors. The bands show the systematic errors from normalization and the number of participants, added in quadrature.

dependence of $dN/d\eta$, shown in Figure 2, is analyzed with the function $dN/d\eta = A \times N_{part} + B \times N_{coll}$, and PHENIX finds that a significant fraction of the particle production scales as N_{coll}. This fraction increases with centrality from $\approx$ 30% at $N_{part} = 68$ to $\approx$ 50% for central collisions.[2] However, the mean transverse energy per charged particle of $\approx$ 0.8 GeV is nearly independent of collision centrality (within a systematic uncertainty of 12 %), and remains very similar to that observed at lower energy at the SPS.[6]. It would be surprising, indeed, if a large admixture of a very different production process left the charged particle spectra nearly identical.

PHENIX finds that $dE_T/d\eta$ for central collisions is 578^{+26}_{-39} GeV at RHIC, about 40 % higher than at the SPS.[6] A straightforward derivation of the energy density can be made, following the method pioneered by Bjorken, assuming longitudinal expansion of the system at the velocity of light. The energy density, ϵ, from our measured value of E_T is at least 4.6 GeV/fm^3, well in the region where deconfinement is expected and more than 50 % higher than achieved at the SPS.

A. Identified Hadrons

The integrated yields of pions, kaons, protons and antiprotons was determined as function of collision centrality.[3] Systematic uncertainties in the absolute normalizations are 13%, 15% and 14% in the measured dN/dy for π, K and (anti)p, respectively.

PHENIX observes a striking 20 antiprotons per unit rapidity in central Au + Au collisions. This is the highest antibaryon density yet reported, and leads one to expect significant production of antinuclei at RHIC. Indeed, antinuclei have been reported by STAR.[7] After conversion to $dN/d\eta$, the sum of the identified charged hadrons agrees with the published PHENIX $dN_{ch}/d\eta$ within 5%.

Hadron yields per participant as a function of N_{part} are shown in Fig. 3. The error bars include statistical and multiplicity dependent systematic errors, while the normalization uncertainty common to all particles gives bands around the positive hadron points. For all particle species, the yield per participant increases with N_{part}. However, the pion yield increases by only $\approx$ 20%, while the kaons and protons rise faster with centrality than the pions ($\approx$ 90%, 65%, 60%, and 70% for K^+, K^-, p and $\overline{p}$, respectively). As jet fragmentation does not tend to favor protons or kaons

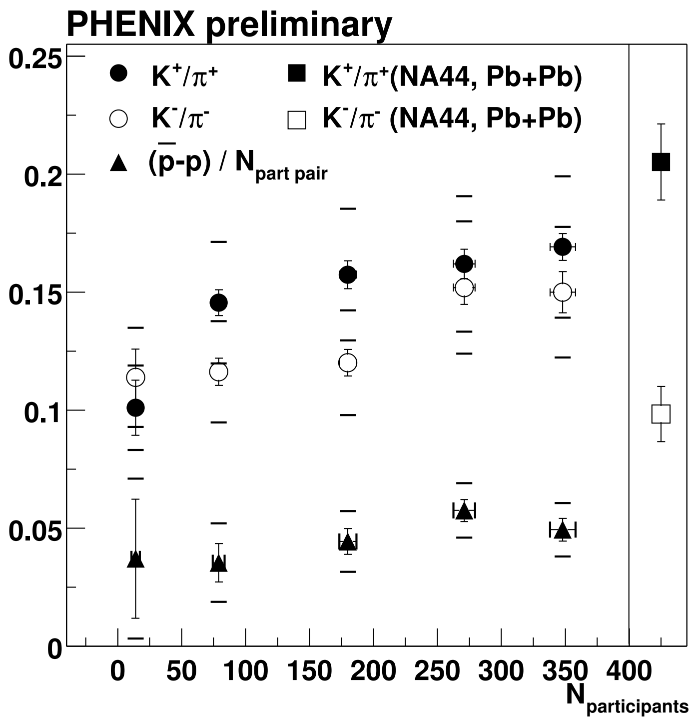

FIG. 4: K/π as a function of the number of participant nucleons in Au+Au collisions at RHIC are shown as closed and open circles for positive and negative charges, respectively. The result for central Pb+Pb collisions at CERN is shown as squares, for comparison. The error bars show statistical errors, while the systematic uncertainties are given by the horizontal bar pairs. Triangles indicate the net baryon rapidity density per participant.

as leading particles, this non-scaling with N_{part} need not indicate production via hard processes. The observed pbar/p ratio of 0.7 suggests that baryon/anti-baryon pair production is the dominant source of protons and anti-protons, rather than the initial nucleons. At $\sqrt{s} = 130$ GeV, such pair production is energetically possible well beyond the first collision suffered by each nucleon. Of course, other observables point to thermal hadron production, so pair production in nearly independent nucleon-nucleon collisions is unlikely to be the correct mechanism in central nuclear collisions at RHIC. Nevertheless scaling of hadron production with participating nucleon number or the number of binary nucleon-nucleon collisions remains a useful analysis tool. The number of net baryons per participant increases by 50% from peripheral to central collisions, but remains less than 1/3 of that observed in central Pb+Pb[8] at the SPS.

Fig. 4 shows the K/π ratio as a function of N_{part}. K^+/π^+ and K^-/π^- both increase with centrality from approximately 10% as was observed in $p-\overline{p}$ collisions at $\sqrt{s} = 200$ GeV to approximately 15%. Positive and negative kaon production does not diverge significantly in central collisions at RHIC as it does in lower energy heavy ion collisions, shown as the open and closed squares. This is almost certainly due to the lower net baryon density at RHIC, as increased baryon density favors K^+ production. The net baryon rapidity density per participant nucleon is also plotted, the value is considerably lower than observed at CERN.

III. IDENTIFIED HADRON SPECTRA

The hadron distributions were plotted as a function of transverse mass ($m_T = \sqrt{p_T^2 + m_0^2}$), and fitted with an exponential for $m_t - m_0 \leq 1.0$ GeV. Low momentum pions were excluded from the fits to avoid contamination by pions arising from resonance decays. The inverse slopes from the fits increase with increasing rest mass of the hadrons; the same systematics were observed at lower energy[9–11] and interpreted as evidence of collective radial expansion in the collisions. Using the simple parameterization

$$T_{eff} = T_{fo} + m < \beta_{radial} >^2$$

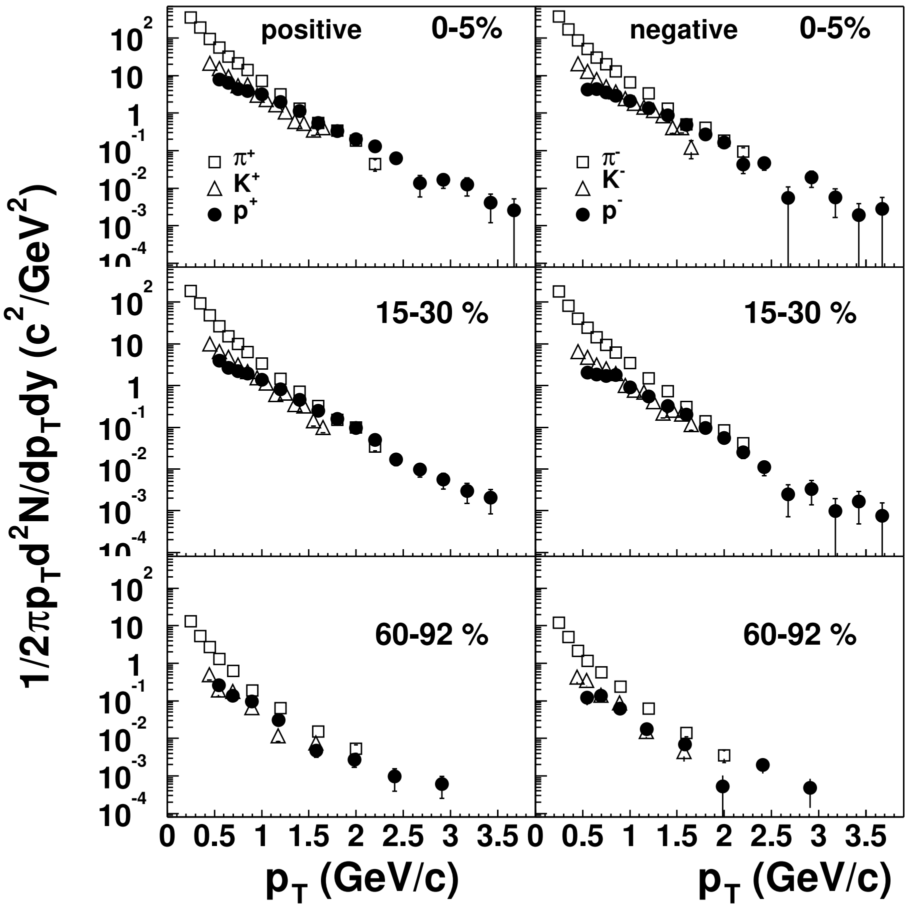

FIG. 5: Transverse momentum spectra of $\pi^{+,-}$, $K^{+,-}$, p, and $\overline{p}$. Positive particles are on the left, negative on the right. Central collisions are in the top section, semi-central in the middle, and peripheral collisions at the bottom; the percentage of the total cross section selected is indicated in each panel.

to separate the freeze-out temperature from radial flow in the spectra, the PHENIX data yield a freeze-out temperature of approximately 140 MeV and $< \beta_{radial} >$ of approximately 0.5. The radial flow velocity in peripheral collisions is significantly lower. The stronger mass dependence of the spectral slopes indicates more explosive collisions at RHIC than at SPS.

This prescription is, however, an oversimplification as the spectra are exponential in m_T over an even smaller momentum range at RHIC than at lower energy. A better way to determine the freezeout parameters is to simultaneously fit all spectra with a parameterization of distributions arising from a hydrodynamically expanding hadron gas. As an intermediate step, we study the centrality dependence of the hadron mean transverse momenta, with no momentum cut applied. PHENIX observes that the $< p_T >$ increases from very peripheral to semi-peripheral collisions, then saturates for pions and kaons. For protons and anti-protons, $< p_T >$ continues to rise with centrality.[3] This general trend is expected to arise from radial flow of the hadrons, but also from multiple scattering at the partonic level and in the gas of gluon saturation in the initial state.[12] Thus, it is impossible to answer from the spectra alone whether the observed centrality dependence is an initial or final state effect.

Another observable sensitive to both the temperature of the system and collective motion is the correlation between identical particles. PHENIX has measured correlations of π^+ and also π^- pairs.[13] We find that the space-time extent of the particle source at freeze-out (i.e. the source radius parameters) are smaller than one would expect from the very explosive nature of the collisions at RHIC. In agreement with the results from STAR,[14] PHENIX finds that the radius parameters are 5-6 fm. The transverse momentum dependence of the extracted radii are very similar to those observed at lower energies at the SPS and AGS. The results agree qualitatively with expectations from a large radial flow, but have not been successfully understood quantitatively with any theory. Hydrodynamic calculations which successfully reproduce the single particle distributions overpredict the magnitude of the radius parameters by a large amount. Furthermore, they cannot reproduce the transverse momentum dependence of the radii.

Figure 5 shows the $\pi^{+,-}, K^{+,-}, p$ and $\overline{p}$ transverse momentum spectra in peripheral, semi-central, and central collisions. In peripheral collisions, the pion spectra exhibit a concave shape which is well described by a power-law parameterization as observed in hadron-hadron collisions. With increasing centrality the curvature in the spectra decreases, leading to a nearly exponential p_T spectrum in central collisions. The kaon spectra change somewhat less visibly. The proton and antiproton spectra become flatter with increasing centrality, leading to the $< p_T >$ systematics described above. A new feature observed for the first time at RHIC is that in central collisions at $p_T \approx 2$ GeV/c the anti-proton yields are comparable to the negative pion yields. Positive and negative hadrons behave in a similar way. For more peripheral collisions, this happens at higher p_T, while in pp and p$\overline{p}$ collisions they never meet. $\overline{p}/\pi^-$ steadily increases with p_T up to ≈ 0.33 at $p_T = 1.5$ GeV/c, nearly independent of $\sqrt{s}$. Different theoretical explanations have been proposed to describe this behavior in heavy ion collisions. Hydrodynamic expansion, perhaps combined with hadronic rescattering, produces such a baryon dominance at high p_T.[15–17] Other explanations include the baryon-junction producton mechanism[18] and gluon saturation[12] in heavy ion collisions.

IV. HARD PROBES

The first hard probe examined at RHIC is the yield of hadrons at large p_T. At sufficiently high p_T the hadrons are dominantly leading particles from the fragmentation of jets. These particles provide a probe of the early time in the collision through their dependence on the amount of matter the partons traverse before fragmenting into jets. Of particular interest is to search for evidence of energy loss via jet quenching in dense matter existing early in the collision.[4] Such energy loss by gluon bremsstrahlung would have many observable consequences, with the most directly measurable being a depletion in yield of high p_T hadrons.

PHENIX measures the spectra to high p_T of both charged hadrons and neutral pions.[19] For the charged particle analyses, the reach in p_T is achieved by removing the particle identification requirements. Only the drift chamber and pad chambers are used; the outer pad chamber match rejects background not originating from the collision vertex. The spectra reach 6 GeV/c p_T, limited by statistics and the background, which reaches 1:1 at 6 GeV/c. The momentum resolution is 3.6% $\oplus$ 0.6%. Neutral pions are measured in the central arms via their $\pi^0 \to \gamma\gamma$ decay. Two separate analyses are performed, using a lead-scintillator (PbSc) sampling calorimeter and a lead-glass Cerenkov (PbGl) calorimeter. The two analyses have very different systematics, and Figure 6 shows the agreement of their final π^0 spectra. Both π^0 spectra have been corrected for losses due to energy resolution, cluster overlaps, analysis cuts, dead detector areas and acceptance; the energy scale of the calorimeters is known to better than 1.5%.

In Figure 6, the data are compared to the binary-collision scaled yield from nucleon-nucleon collisions. We parameterize the cross section $1/(2\pi p_T)d^2\sigma/d\eta dp_T$ for N+N $\to (h^+ + h^-)/2$ as $A/(1+p_T/p_0)^n$, with A $= 330$ mb/GeV^2/c^2, $p_0 = 1.72$ GeV/c and n=12.4. These parameters were determined by interpolating between charged hadron production in $p-p$ collisions at the ISR and $\overline{p}-p$ collisions from UA1 at CERN and CDF at FNAL. The number of collisions is calculated using a Glauber model.

For $p_T > 2$ GeV/c the binary-scaling prediction agrees quite well with the data from peripheral collisions for both charged and neutrals. In central collisions, however, the data lie noticeably below the prediction for both. To examine this difference more directly, we plot the ratio R_{AA} for central collisions in Figure 7. R_{AA} is the ratio of the yield per event in A+A collisions per binary nucleon-nucleon collision to the yield in N+N collisions. The π^0 spectra are a weighted average of the PbSc and PbGl results. For the charged spectrum, R_{AA} rises up to 2 GeV/c as expected from the soft processes discussed above. But above 2 GeV/c, R_{AA} remains significantly below unity for both spectra.

The depletion is quite striking since the production of high p_T hadrons in p+A collisions is known to be enhanced compared to the binary-scaling expectation for $p_T > 2$ GeV/c.[20] A similar enhancement has been observed in heavy ion collisions at lower energies,[21, 22] as shown in Figure 7. Above 2 GeV/c R_{AA} is lower for pions than for charged hadrons, which implies that the π/h ratio is smaller in central RHIC Au+Au collisions than in ISR p+p collisions. This is consistent with the identified charged hadron results.

The suppression in central collisions is in qualitative agreement with the predictions of energy loss by scattered partons traversing a dense medium,[4] but other explanations cannot be ruled out at this time. One possible explanation could be nuclear shadowing of the parton distribution, which would decrease the number of hard scatterings to begin with. To investigate this, we can estimate the momentum fraction carried by the struck partons at RHIC and compare to the lower energy data. As the hadron p_T values are modest, their most probable (hard-scattering) source

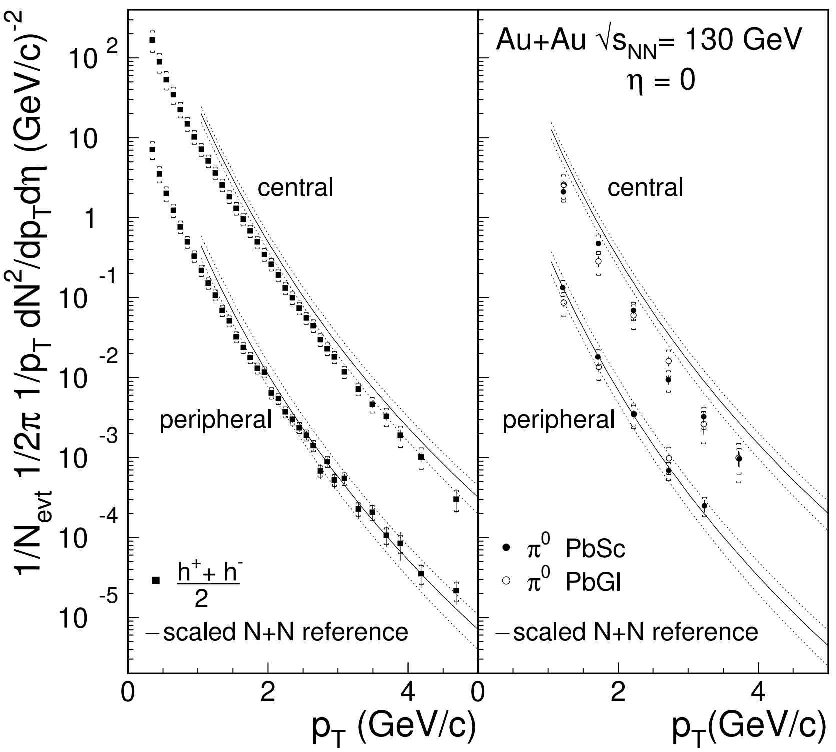

FIG. 6: Midrapidity yields of charged hadrons (left) and neutral pions (right) as a function of p_T for 60-80% peripheral and 0-10% most central collisions. The π^0 results from PbSc and PbGl are plotted separately. The error bars indicate the statistical uncertainties, while the surrounding brackets show systematic errors. Shown for reference are the yields in N+N collisions, scaled up by the number of binary collisions for each centrality class. The bands indicate uncertainties in the N+N reference spectrum and the determination of $< N_{binary} >$.

is low momentum jets which fragment into a very small number of hadrons. For single hadron fragmentation of jets at y=0, the momentum fraction can be calculated exactly using $x_T = 2p_T/\sqrt{s}$. For the CERN SPS and ISR data, $x_T = 0.2 - 0.4$, while at RHIC $x_T = 3 - 5 \times 10^{-2}$. For fragmentation into a small number of hadrons, the x values are somewhat higher. The momentum fraction carried by the partons struck in RHIC collisions is still rather large compared to the x range where gluon shadowing is predicted to be significant.[23] This conclusion is supported by comparison to observed nuclear shadowing of quark distributions, evolved to comparable values of Q^2.[23] Thus, the depletion is unlikely to arise from nuclear shadowing. Nevertheless, further measurements at RHIC, including spectra in p+A collisions, higher p_T reach and correlations, will be necessary to pin down the source of the depletion.

V. ELECTRONS IN PHENIX

PHENIX has made a first measurement of single electron spectra in Au+Au collisions.[24] The measurement of single leptons at $p_T \geq 1.0$ GeV/c is a useful way to study heavy quark production and probe the hot, dense matter early in the collision. Charm production is sensitive to the initial state gluon density, as gluon fusion is the dominant heavy quark production mechanism at this $\sqrt{s}$. Measurement of charm production is also crucial for understanding J/ψ suppression, which was proposed as a signal of the deconfinement phase transition.[25] The dilepton mass distribution between 1 and 3 GeV invariant mass contains a large contribution from charm decays, and the single lepton spectrum also is sensitive to open charm.

Electrons are identified in PHENIX by projecting tracks reconstructed in the drift chamber into the Ring Imag-

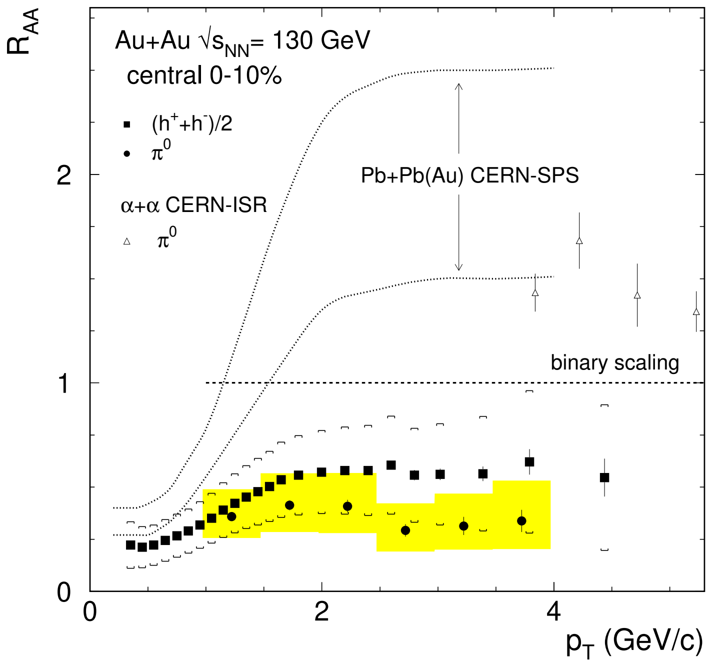

FIG. 7: The ratio R_{AA} for charged hadrons and neutral pions (combining PbSc and PbGl results) in central Au+Au collisions. The error bars indicate statistical errors. The surrounding bands (shaded for π^0, brackets for charged) are the quadrature sums of (i) the systematic errors on the measurement, (ii) the uncertainty in the p+p data, and (iii) the uncertainty in $< N_{binary} >$. Also shown for reference are the ratio of inclusive cross sections in $\alpha - \alpha$ compared to p-p at $\sqrt{s_{NN}} = 31$ GeV (ISR) and semi-inclusive spectra from heavy ion collisions at $\sqrt{s_{NN}} = 17$ GeV/A (SPS). The latter combines several experiments and is shown as a band to indicate the range of uncertainties in the SPS data.

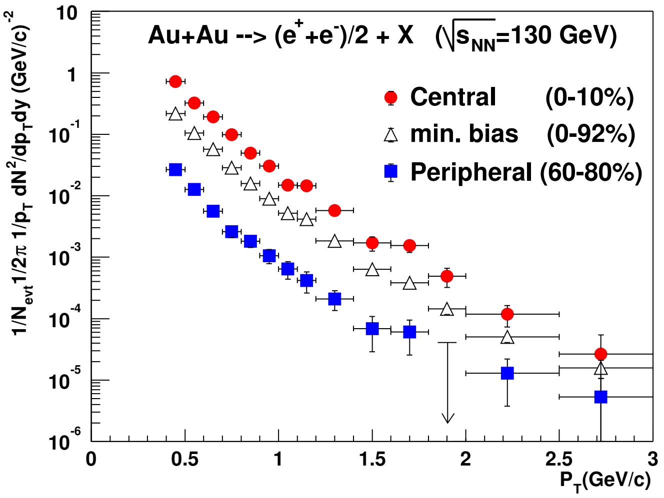

FIG. 8: The transverse momentum spectra of electrons and positions $(e^+ + e^-)/2$ from central, peripheral and minimum bias Au+Au collisions.

ing Cerenkov phototube array and associating the tracks with energy measured in the electromagnetic calorimeter. The calorimeter energy resolution is $8.2\%/\sqrt{E(GeV)} \oplus$ 1.9 %. Electron candidates must have at least three RICH phototubes within a distance characteristic of an electron track. Low values of E/p are rejected to remove remaining hadrons. Remaining background due to accidental associations is measured statistically by event mixing, and is subtracted from the yield. The systematic uncertainty on the electron momentum distribution is approximately 11%.

Figure 8 shows the p_T distributions of electrons in PHENIX for central, minimum bias, and peripheral collisions. The expected sources of electrons are a) Dalitz decays of $\pi^0, \eta, \eta\prime, \omega$, and ϕ; b) di-electron decays of ρ, ω, and ϕ; c) photon conversions; d) kaon decays; e)semi-leptonic decays of charm; f)bottom decays and thermal dileptons. The first four sources are considered "background" for the single electron measurement and are calculated with a hadron event generator tuned to reproduce the measured PHENIX pion spectrum. We observe a significant excess of single electron yield above these sources in minimum bias and central collisions.[24] Adding charm and bottom decays to the generator results in agreement with the measured spectra. From this comparison we can extract the charm cross section per binary nucleon-nucleon collision. This is found to be in approximate agreement with the value from PYTHIA tuned to reproduce charm production observed at the ISR, SPS and FNAL. However, the error bar from this measurement is very large, precluding any significant conclusion yet. Higher statistics, electron-positron pair yields, and a measurement in p-p collisions at the same $\sqrt{s}$ will be required; these measurements are currently underway.

VI. CONCLUSION

PHENIX has shown that the energy density reached at RHIC is at least 4.6 GeV/fm^3. The yield of kaons and protons per participating nucleon increases in central collisions. The hadron spectra are consistent with a large radial collective expansion, which extends the transverse momentum range dominated by soft processes to 3 GeV/c. The baryons and antibaryon yields become equal to those of pions at $p_T \geq 2$ GeV/c. However, the two-particle correlations are nearly identical with those in lower energy collisions, providing a mystery and a challenge to hydrodynamical models of the collision dynamics.

We observe a *deficit* of particle production at high p_T, compared to yields expected by scaling nucleon-nucleon collisions. The deficit is larger for pions than for all charged hadrons, which is consistent with the baryon and pion spectral shapes. The deficit is almost certainly not a result of nuclear shadowing of the initial parton distributions. However, further measurements are needed for an unambiguous conclusion whether this is a signal of parton energy loss in dense matter. PHENIX has also made a first measurement of leptons at RHIC. We see a significant contribution from open charm decays.

The data collected in run2 of RHIC will allow to extend the p_T range to at least 10 GeV/c, study correlations of high p_T particles, and measure J/ψ and direct photon yields. Furthermore, we will measure p-p collisions in the same detector.

[1] H. Hamagaki et al. (PHENIX Collaboration) Nucl. Phys. A698, 412 (2002).
[2] K. Adcox et al. (PHENIX Collaboration), Phys. Rev. Lett. 86, 3500 (2001).
[3] K. Adcox et al (PHENIX Collaboration), nucl-ex/0112008.
[4] X.N. Wang and M. Gyulassy, Phys. Rev. Lett. 68, 1480 (1992); X.N. Wang, Phys. Rev. C58, 2321 (1998).
[5] D. Kharzeev and M. Nardi, Phys. Lett. B507, 121 (2001).
[6] K. Adcox et al. (PHENIX Collaboration), Phys. Rev. Lett. 87, 052301 (2001).
[7] C. Adler et al. (STAR Collaboration), Phys. Rev. Lett. 87, 262301 (2001).
[8] I.G. Bearden, et al. (NA44 Collaboration), Phys. Lett. B388, 431 (1996).
[9] I.G. Bearden et al. (NA44 Collaboration), Phys. Rev. Lett. 78, 2080 (1997).
[10] H. Appelshauser et al., Eur. Phys. J. C2, 661 (1998).
[11] L. Ahle et al. (E802 Collaboration), Nucl. Phys. A638, 57c (1998).
[12] J. Schaffner-Bielich, D. Kharzeev, L. McLerran, and R. Venugopalan, nucl-th/0108048, (2001).
[13] K. Adcox et al (PHENIX Collaboration), nucl-ex/0201008 (2002).
[14] C. Adler et al. (STAR Collaboration), Phys. Rev. Lett. 87, 082301 (2001).
[15] D. Teaney et al., Phys. Rev. Lett. 86, 4783 (2001); nucl-th/0110037.
[16] P. Kolb et al. Nucl. Phys. A696, 197 (2001); P. Huovinen et al., Phys. Lett. B503, 58 (2001).
[17] W. Broniowski and W. Florkowski, nucl-th/0106050.
[18] S.E. Vance and M. Gyulassy, Phys. Rev. Lett. 83, 1735 (1999).
[19] K. Adcox et al. (PHENIX Collaboration), Phys. Rev. Lett. 88, 022301 (2002).
[20] D. Antreasyan et al., Phys. Rev. D19, 764 (1979).

[21] E.Wang and X.N. Wang, Phys. Rev. C64, 034901 (2001), and references therein.
[22] A.L.S. Angelis et al., Phys. Lett. B185, 213 (1987).
[23] Z. Huang, H.J. Lu and I. Sarcevic, Nucl. Phys. A637, 79 (1998).
[24] K. Adcox, et al. (PHENIX Collaboration), nucl-ex/0202002 (2002).
[25] T. Matsui and H. Satz, Phys. Lett. B178, 416 (1986); M.C. Abreu et al., Phys. Lett. B447, 28 (2000).